International Journal of Heat and Mass Transfer 112 (2017) 1113–1121

Contents lists available at ScienceDirect

International Journal of Heat and Mass Transfer

journal homepage: www.elsevier.com/locate/ijhmt

# An experimental study to determine the maximum efficiency index in turbulent flow of $SiO_2$/water nanofluids

Chaiwat Jumpholkul [a], Omid Mahian [b], Alibakhsh Kasaeian [c], Ahmet Selim Dalkilic [d], Somchai Wongwises [a,e,*]

[a] Fluid Mechanics, Thermal Engineering and Multiphase Flow Research Laboratory (FUTURE), Department of Mechanical Engineering, Faculty of Engineering, King Mongkut's University of Technology Thonburi, Bangmod, Bangkok, Thailand
[b] Renewable Energies, Magnetism and Nanotechnology Lab., Faculty of Science, Ferdowsi University of Mashhad, Mashhad, Iran
[c] Faculty of New Sciences and Technologies, University of Tehran, Tehran, Iran
[d] Heat and Thermodynamics Division, Department of Mechanical Engineering, Yildiz Technical University, Yildiz, Istanbul 34349, Turkey
[e] The Academy of Sciences, Royal Society of Thailand, Sanam Suea Pa, Dusit, Bangkok 10300, Thailand

ARTICLE INFO

*Article history:*
Received 11 February 2017
Received in revised form 30 April 2017
Accepted 2 May 2017

*Keywords:*
Efficiency index
$SiO_2$/water nanofluid
Heat transfer
Pressure drop
Turbulent flow

ABSTRACT

In this work, heat transfer and pressure drop characteristics of nanofluids flowing through a horizontal circular tube have been investigated experimentally. The test tube was made of stainless steel type 304 with an inner diameter of 7.1 mm. The working fluid was $SiO_2$/water nanofluid where the average diameter of nanoparticles was 7 nm. Nanofluids at three different volume concentrations of 0.5, 1, and 2% have been prepared and tested. The experiments have been performed for Reynolds numbers ranging from 3800 to 12000, inlet temperatures of 25, 30, and 35 °C where a constant heat flux was imposed on the tube. The effects of particle volume concentrations, inlet temperature and mass flow rate on convective heat transfer and pressure drop characteristics have been evaluated. The results revealed that with increasing Reynolds number, volume concentration, and inlet temperature the heat transfer coefficient and Nusselt number increased. Moreover, pressure drop increased with increasing volume concentration; conversely, decreased with increasing inlet temperature. The efficiency index reached its maximum quantity (i.e. 1.6) at Reynolds numbers higher than 9000, the volume concentration of 2%, and inlet temperature of 35 °C. On the other hand, the minimum values of efficiency index were obtained for Reynolds numbers less than 7000, the volume fraction of 0.5%, and inlet temperature of 25 °C. Finally, new correlations for predicting the Nusselt number and friction factor of $SiO_2$/water turbulent flow have been proposed.

© 2017 Elsevier Ltd. All rights reserved.

## 1. Introduction

During last decades, many researchers strived to ameliorate efficiency of thermal systems through various heat transfer enhancement techniques. These techniques have been applied to the design of heat exchangers which are widely utilized in different industries. Many methods have been suggested to promote the performance of heat exchangers. Among the proposed techniques for heat transfer enhancement, usage of nanofluids instead of conventional working fluids has attracted special attention. Nanofluids are relatively a new type of working fluids which are produced by dispersion of solid nanoparticles in conventional liquids through implementing special chemical and physical processes. In comparison with microsuspensions, nanosuspensions have special privileges such as higher thermal conductivity, long-term stability, and less clogging in conduits. Numerous review and research reports have been published on the preparation and properties, flow characteristics, and applications of nanofluids in diverse systems such as solar collectors, solar stills, photovoltaic thermal systems and so on [1–18].

Up to now, noticeable attempts have been made to determine the flow and heat transfer characteristics of various nanofluids in plain tubes; because, despite the simple configuration, they have the most application in industries. Here, a brief review of some of these works has been presented.

Pak and Cho [19] investigated the friction and heat transfer characteristics of nanofluids in turbulent flow. Two different types of metallic oxide nanoparticles, alumina and titanium dioxide, with mean diameters of 13 and 27 nm, respectively, were tested. The results showed that the Nusselt number of nanofluids

* Corresponding author at: Fluid Mechanics, Thermal Engineering and Multiphase Flow Research Laboratory (FUTURE), Department of Mechanical Engineering, Faculty of Engineering, King Mongkut's University of Technology Thonburi, Bangmod, Bangkok, Thailand.
*E-mail address:* somchai.won@kmutt.ac.th (S. Wongwises).

http://dx.doi.org/10.1016/j.ijheatmasstransfer.2017.05.007
0017-9310/© 2017 Elsevier Ltd. All rights reserved.

**Nomenclature**

| | |
|---|---|
| A | surface area of test section ($m^2$) |
| Cp | specific heat at constant pressure (J/kg K) |
| $D_i$ | inside tube diameter (m) |
| d | diameter (m) |
| f | friction factor |
| h | heat transfer coefficient ($W/m^2$ K) |
| I | electric current (A) |
| k | thermal conductivity (W/m K) |
| L | length of test section (m) |
| $\dot{m}$ | mass flow rate (kg/s) |
| *Nu* | Nusselt number |
| *Pr* | Prandtl number |
| Q | heat transfer rate (W) |
| *Re* | Reynolds number |
| r | radius (m) |
| T | temperature (°C) |
| u | velocity (m/s) |
| V | electric voltage (V) |

*Greek symbol*

| | |
|---|---|
| $\alpha$ | thermal diffusivity ($m^2/s$) |
| $\varepsilon$ | tube roughness (m) |
| $\eta$ | efficiency index |
| $\mu$ | dynamic viscosity (kg/m s) |
| $\phi$ | volume concentration (%) |
| $\rho$ | density ($kg/m^2$) |
| $\Delta P$ | pressure drop (Pa) |

*Subscripts*

| | |
|---|---|
| ave | average |
| bf | base fluid |
| in | inlet |
| nf | nanofluids |
| out | outlet |
| p | particle |
| ss | stainless steel |
| sup | supply |
| wi | inner wall |
| wo | outer wall |

increased with increasing volume concentration beyond Reynolds number. Finally, a new correlation for predicted turbulent convective heat transfer coefficient of nanofluids was proposed.

Xuan and Li [20] studied convective heat transfer and flow characteristics of Cu-water nanofluids flowing through a circular tube. Their results showed that the mixture remarkably gives a higher heat transfer coefficient compared to water while there is no significant change in friction factor. Finally, a new correlation for convective heat transfer was proposed.

Duangthongsuk and Wongwises [21] conducted an experimental study to determine the ability of $TiO_2$/water nanofluids (volume fractions between 0.2 and 2% and mean particle diameter of 21 nm) for heat transfer enhancement in a double tube heat exchanger. Their study elucidated that using nanofluid with a volume fraction of 1% instead of water can augment heat transfer rate as much as 26%. The maximum and minimum heat transfer rates occurred at volume fractions of 1 and 2%, respectively. Moreover, the pressure drop of nanofluids was slightly increased when compared to water and increased with increasing nanofluid concentration.

Abbasian Arani and Amani [22] evaluated the impact of nanoparticles size on the turbulent flow characteristics of nanofluids. Titanium dioxide nanoparticles with average sizes of 10, 20, 30 and 50 nm were dispersed in DI-water as the base liquid. The results showed that the maximum performance index (i.e. 1.9) could be achieved by using nanoparticles with a mean diameter of 20 nm where the concentration is 2 vol.%.

Karimzadehkhouei et al. [23] investigated pressure drop and heat transfer characteristics of water-based nanofluids in horizontal smooth hypodermic microtubes. Two different types of nanoparticles $TiO_2$ and $Al_2O_3$ with an average diameter of 20 nm were added to DI-water to prepare nanofluids with mass fractions of 0.01–3 wt.%. Their results showed that there is no significant heat transfer enhancement for $Re < 1000$. However, at higher Reynolds numbers, heat transfer enhancement was reported. Under these conditions, the enhancement in heat transfer increased with nanoparticle mass fraction.

Kulkarni et al. [24] experimentally studied the heat transfer and fluid dynamic performance of silicon dioxide ($SiO_2$) nanoparticles with three different sizes including 20, 50 and 100 nm suspended in a 60:40 (% by weight) ethylene glycol and water mixture. They found that the increase in particles diameter increased the heat transfer coefficient. Their experimental results also revealed that the pressure drop increased with increasing volume concentration.

Vajjha et al. [25] experimentally investigated flow and heat transfer characteristics of three nanofluids in a circular tube under turbulent regime. The results showed that heat transfer coefficient and pressure loss increased with particle volume fraction. Finally, new correlations for Nusselt number and friction factor were proposed.

Ferrouillat et al. [26] studied the heat transfer and pressure drop of nanofluids flowing through a smooth tube under constant wall temperature condition. Silica/water nanofluids at concentrations of 2.31, 7.95 and 18.93 vol.% were tested. Results indicated that heat transfer coefficient could be augmented up to 60% compared to pure water whereas pressure drop slightly increased compared to water. Later, Ferrouillat et al. [27] studied the effects of two types and shapes of water-based nanofluids on heat transfer. Spherical and "banana-like" shapes were studied for $SiO_2$ suspensions. Polygonal and rod-like were used for ZnO nanofluids. The results revealed that Nusselt number increased only slightly compared to the use of water as the working fluid.

Azmi et al. [28] experimentally investigated the heat transfer coefficient and friction factor of $SiO_2$/water nanofluids up to 4 vol. % having a mean particle diameter of 22 nm flowing in a circular tube under constant heat flux boundary condition. The experiments were undertaken in the Reynolds number range of 5000–27,000 at a bulk temperature of 30 °C. The results showed that heat transfer coefficient increased with volume concentration up to 3.0% and decreased after that. In 2016, Azmi et al. [29] studied the effects of different operating temperatures on forced convection heat transfer of $TiO_2$/water-ethylene glycol nanofluids in a circular tube under turbulent flow regime. The results showed that Nusselt number increased up to 22.8% and 28.9% for temperatures of 50 °C and 70 °C, respectively. Moreover, friction factor of nanofluids was slightly increased with concentration.

Merilainen et al. [30] carried out experimental studies of turbulent convective heat transfer of water-based nanofluids having different types of nanoparticles including $Al_2O_3$ (8.2 ± 3.1 and 14–53 nm), $SiO_2$ (6.5 ± 1.8, 65 ± 34 and 28–100 nm), and MgO (21 ± 10 and 15–47 nm). Their data showed that nanofluids heat transfer coefficient could be enhanced up to 40% compared to the base fluid. By considering the simultaneous variations in heat

**Table 1**
Characteristics of $SiO_2$ nanoparticles.

| Mean diameter (nm) | Density ($kg/m^2$) | Thermal conductivity (W/m K) | Specific heat (J/kg K) | Thermal diffusivity ($m^2/s$) |
|---|---|---|---|---|
| 7 | 2200 | 1.4 | 765 | $0.834 \times 10^{-6}$ |

transfer enhancement and pressure drop, they concluded that only $SiO_2$ nanoparticles with an average size 6.5 ± 1.8 nm and volume concentrations between 0.5 and 2% are advantageous to use.

Martinez-cuenca et al. [31] examined the forced convective heat transfer and pressure drop of $SiO_2$, $Al_2O_3$ and MWCNTs water-based nanofluids. The results indicated that at a given Reynolds number, heat transfer coefficient increased compared to water, but at a given pumping power, opposite trends were observed. Some researchers [32–34] demonstrated that further correlations are required to predict the heat transfer and fluid flow of nanofluids since conventional single-phase correlations are not appropriate.

As mentioned above, most of the experimental studies dealt with nanofluids having alumina ($Al_2O_3$) and titanium dioxide ($TiO_2$) nanoparticles, and there are few experimental data on flow and heat transfer of nanofluids having $SiO_2$ nanoparticles although this type of particles is one of the cheapest nanoparticles. In addition, based on the best knowledge of authors, for very small nanoparticles (less than 10 nm) there are a few data in the current literature (only in the work of Merilainen et al. [30]). The main aim of this study is to determine the efficiency index of $SiO_2$/water nanofluids where the size of nanoparticles is just 7 nm. In this study, effects of different volume concentrations and inlet temperatures of $SiO_2$/water nanofluids on the heat transfer coefficient, pressure drop, and efficiency index are investigated in turbulent flow. Finally, based on the experimental results, new heat transfer and friction factor correlations of $SiO_2$/water nanofluids are proposed.

## 2. Sample preparation

One of the main obstacles encountered in nanofluids experiments is the agglomeration of particles. Preparation of nanofluids is a very important step in applying nanoparticles for improving the heat transfer characteristics of conventional fluids. Xuan and Li [20] suggested the methods used for stabilizing the suspensions such as changing the pH value of suspension, adding the surfactant and using ultrasonic vibration. In the present study, silicon dioxide ($SiO_2$) nanoparticles with a mean diameter of 7 nm (Aerosil 380) were purchase from Degussa. DI-water was added to the concentrated nanofluids and careful mass measurement of the resulting fluid in the electronic mass balance was conducted to arrive at the desired particles volume concentrations of nanofluids of 0.5, 1 and 2% without any surfactant. Before using the nanofluids sample for measurement, it was subjected to an ultrasonic bath for 2 h to ensure proper dispersion of the nanoparticles. The characteristics of nanoparticles used in this study are summarized in Table 1.

## 3. Experimental apparatus

The schematic diagram of the experimental apparatus is shown in Fig. 1. The experimental setup consists of test tube made of stainless type 304 length of 2 m, outer and inner diameter of 9.5 and 7 mm. The DC power supply was employed and its voltage was adjusted by the voltmeter to control the heat flux at the pipe wall. Ultrasonic bath model VGT-1990QT with a power of 240 W, and a capacity of 9 L was used as storage tank, which provides more stable nanofluids and reduce sedimentation during tests. Constant temperature tank, with electrical heater, cooling coil and a thermostat were used to keep the nanofluids temperature at the desired level. Two sight glass tubes with an inner diameter equal to the test section were installed before and after the test section to visualize the nanofluids flow and probable nanoparticles sedimentation. In order to measure the wall temperature, 9 T-type thermocouples (with the precision of ±0.1 °C) were mounted at different axial positions on the surface of the test section. Further 2 T-type thermocouples were inserted into the flow at the inlet and outlet of the test section to measure the bulk temperatures of nanofluids. The test section was insulated with fiberglass cloth and rubber insulation to

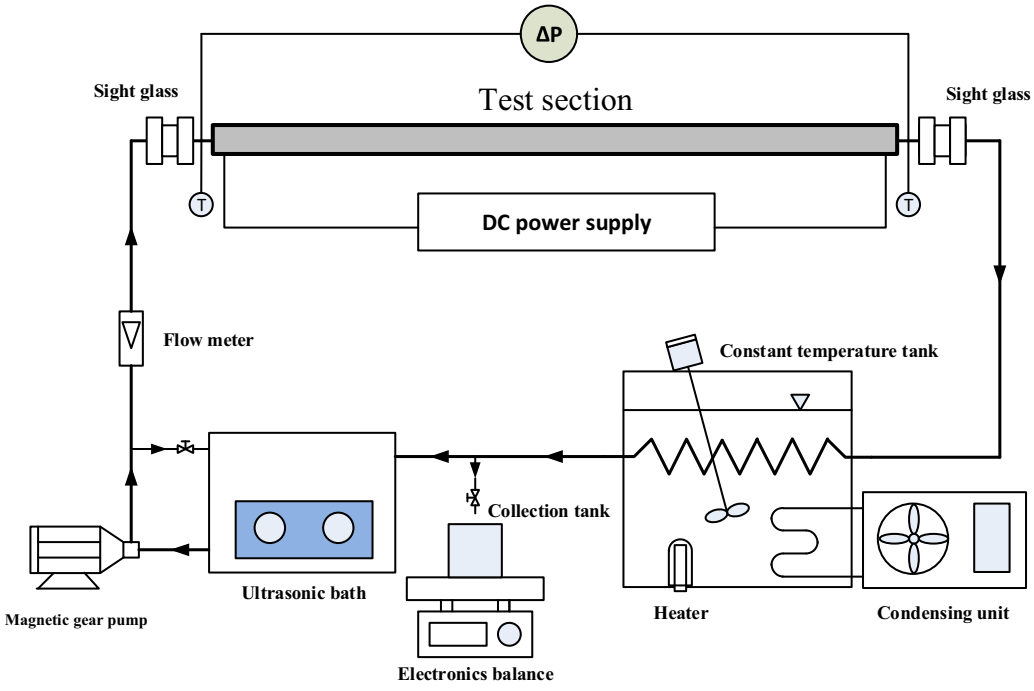


**Fig. 1.** Schematic diagram of the experimental apparatus.

**Table 2**
Uncertainties of instruments and calculated parameters.

| Parameter | Uncertainty |
|---|---|
| Temperature (°C) | ±0.1 |
| Pressure drop (Pa) | ±7 |
| Mass flow rate (kg/s) | ±0.0035 |
| Electric power (W) | ±7.1 |
| Nusselt number | ±8.6% |
| Friction factor | ±0.9% |

prevent heat loss in a radial direction. The nanofluids was forced through the flow loop by magnetic gear pump, which could be adjusted the flow rates by the inverter. Moreover, the nanofluids flow rates were determined by the weighting method. The pressure drop between the inlet and outlet of the test section was measured by using a differential pressure transmitter (YOKOGAWA-EJA110A). When the system reached stable conditions, temperatures recorded using a data logger every 10 min. Water was retested between nanofluids runs in order to ensure that there was no significant fouling due to the particles and, in fact, none was found. The uncertainties of the instruments and calculated parameters are shown in Table 2.

## 4. Data reduction

The heat supplied to the test section can be calculated from:

$$Q_{\sup} = IV \tag{1}$$

where $I$ is the electrical current, and $V$ is the electrical voltage.

The heat transfer rate into the nanofluids is calculated from:

$$Q_{nf} = \dot{m}_{nf} Cp_{nf} (T_{out} - T_{in})_{nf} \tag{2}$$

where $Q_{nf}$ is the heat transfer rate and $\dot{m}_{nf}$ is the mass flow rate of the nanofluids, respectively.

The average heat transfer rate is defined as follows:

$$Q_{ave} = \frac{Q_{\sup} + Q_{nf}}{2} \tag{3}$$

where $Q_{ave}$ is the average heat rate between supply and the nanofluids.

The measured heat transfer coefficient and Nusselt number are calculated from the following equations:

$$h_{nf} = \frac{Q_{ave}}{A_{wi}(T_{wi} - T_{nf})} \tag{4}$$

$$Nu_{nf} = \frac{h_{nf} D_i}{k_{nf}} \tag{5}$$

The outer wall temperatures ($T_{wo}$) were measured by 9 thermocouples installed at the outer wall of the test tube. These outer wall temperatures were used to determine the inner wall temperatures ($T_{wi}$), which can be solved by using the one-dimensional heat conduction equation in cylindrical coordinates as following equations:

$$T_{wi} = T_{wo} - \frac{Q_{ave}\left(\ln \frac{r_o}{r_i}\right)}{2\pi L k_{ss}} \tag{6}$$

where $k_{ss}$ is the thermal conductivity of stainless steel (14.4 W/m K).

The thermo-physical properties such as density, specific heat, viscosity and thermal conductivity of the nanofluids are calculated using the following correlations.

The density is calculated from Pak and Cho [19] as:

$$\rho_{nf} = \phi \rho_p + (1 - \phi)_{bf} \tag{7}$$

The specific heat is calculated from Vajjha and Das [35] as follows:

$$\frac{Cp_{nf}}{Cp_{bf}} = \left( \frac{(0.001769 T_{nf}) + (1.1937)\left(\frac{Cp_p}{Cp_{bf}}\right)}{(0.8021 + \phi)} \right) \tag{8}$$

Sharma et al. [36] developed equations for the estimation of viscosity and thermal conductivity given by Eqs. (9) and (10), respectively, for water-based nanofluids. They are given as:

$$\frac{\mu_{nf}}{\mu_{bf}} = \left(1 + \frac{\phi}{100}\right)^{11.3} \left(1 + \frac{T_{nf}}{70}\right)^{-0.038} \left(1 + \frac{d_p}{170}\right)^{-0.061} \tag{9}$$

$$\frac{k_{nf}}{k_{bf}} = 0.8938 \left(1 + \frac{\phi}{100}\right)^{1.38} \left(1 + \frac{T_{nf}}{70}\right)^{0.2777} \left(1 + \frac{d_p}{150}\right)^{-0.0336} \left(\frac{\alpha_p}{\alpha_{bf}}\right)^{0.01737} \tag{10}$$

The properties of the nanofluids shown in the above equations are evaluated from water and nanoparticles at average bulk temperature.

## 5. Results and discussion

In order to validate the accuracy of the experimental apparatus, the experimental results were compared with the well-known correlations for Nusselt number and friction factor. The measured Nusselt number were compared directly with the correlations proposed by Dittus-Boelter [37], Sleicher-Rouse [38] and Gnielinski [39] given by Eqs. (11)–(13) respectively.

Dittus-Boelter [37]

$$Nu = 0.023\, Re^{0.8}\, Pr^{0.4} \tag{11}$$

Sleicher-Rouse [38]

$$Nu = 5 + 0.015\, Re^{a}\, Pr^{b} \tag{12}$$

where: $a = 0.88 - 0.24/(4 + Pr)$ and $b = 1/3 + 0.5e^{-0.6Pr}$

Gnielinski [39]

$$Nu = \frac{(f/8)(Re - 1000)Pr}{1 + 12.7(f/8)^{0.5}(Pr^{2/3} - 1)} \tag{13}$$

The experimental values of friction factor are compared with correlations of Blasius [40] and Haaland [41] given in Eqs. (14) and (15), respectively.

Blasius [40]

$$f = 0.316\, Re^{-0.25} \tag{14}$$

Haaland [41]

$$\frac{1}{f} = -1.8 \ell og\left( \left(\frac{\varepsilon/D}{3.7}\right)^{1.11} + \frac{6.9}{Re} \right) \tag{15}$$

Figs. 2 and 3 compare the present experimental data on Nusselt number and friction factor with the predicted results from well-known correlations. As seen, there is good agreement between the results for the base fluid and predicted from well-known correlations. It can be concluded that the experimental set-up are accurate.

### 5.1. Convective heat transfer coefficient

This part presents the effect of nanofluids volume concentration and inlet temperature on heat transfer coefficient. $SiO_2$/water nanofluids were used as working fluid flowing through a smooth pipe. The nanofluids used in the experiments had concentration

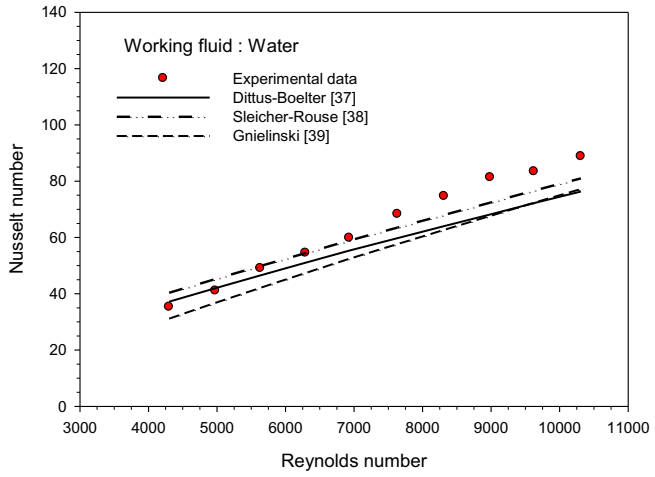


**Fig. 2.** Comparison between measured Nusselt number and that calculated from well-known correlations.

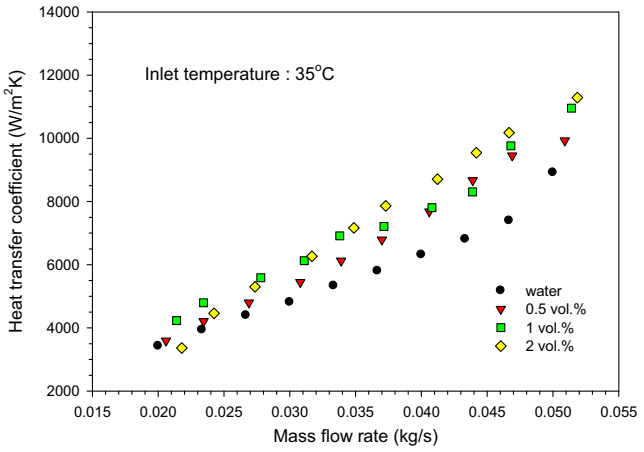


**Fig. 4.** Experimental heat transfer coefficient for water and $SiO_2$/water nanofluids versus Mass flow rate at inlet temperature of 35 °C.

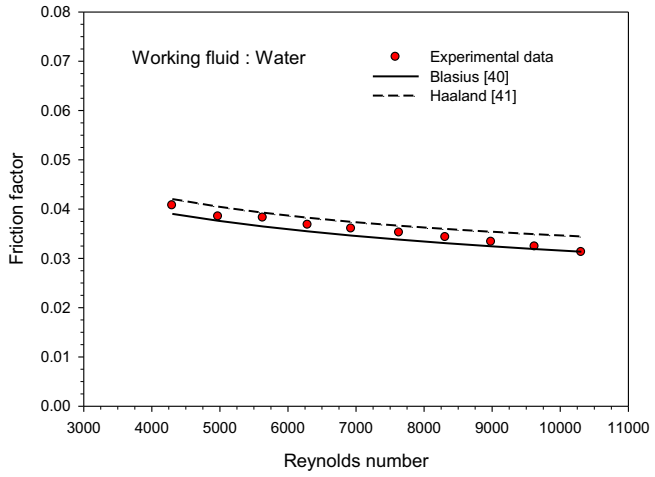


**Fig. 3.** Comparison between measured friction factor and that calculated from well – known correlations.

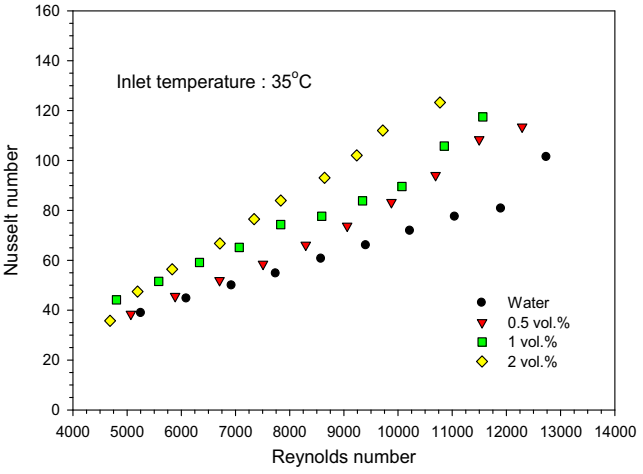


**Fig. 5.** Experimental Nusselt number for water and $SiO_2$/water nanofluids versus Reynolds number at inlet temperature of 35 °C.

levels of 0.5 vol.%, 1 vol.%, and 2 vol.% and inlet temperature of 25 °C, 30 °C, and 35 °C.

Fig. 4 displays heat transfer coefficient in terms of mass flow rate and volume concentration. It can be seen that when mass flow rate increases, the heat transfer coefficient increases because the increase in mass flow rate corresponds to the enhancement of turbulence in fluid flow. When we use a nanofluid instead of water as the working fluid, it will be more complicated to analysis the effect of increases in turbulence intensity on the heat transfer rate, because the motions of nanoparticles have a key role on boundary layer thickness, and, consequently, heat transfer rate. Microconvection induced by Brownian motion of nanoparticles, thermophoresis, and rate of sedimentation are some of phenomena that will be influenced by changes in Reynolds number (or mass flow rate), and, consequently, will affect the heat transfer rate in the channel. It is also seen that, at a given mass flow rate, the increase of volume concentration leads to augmentation in heat transfer coefficient. Heat transfer coefficient has a direct relation with thermal conductivity and an inverse relation with boundary layer thickness. When the nanofluid concentration increases, the effective thermal conductivity of working fluid also increases that this enhances heat transfer rate.

Fig. 5 illustrates the relationship between Nusselt number and Reynolds number at different concentrations. It can be seen from the figure that Nusselt number of nanofluids is higher than that of base fluid and will increase when the volume concentration increases, similar to the heat transfer coefficient. At Reynolds number of 11,000 and concentrations of 2 vol.%, Nusselt number will increase by about 35% compared to the base fluid.

Effects of inlet temperature of nanofluids on Nusselt number are shown in Fig. 6. It can be seen that the inlet temperature has significant effects on Nusselt number. Nusselt number reaches its maximum value at the inlet temperature of 35 °C. This is because, at higher inlet temperature, molecules of both base fluid and nanoparticles have more turbulence, this, in turn, causes more severe collision than at lower inlet temperature which results in better heat transfer.

Fig. 7 depicts the relationship between Nusselt number gained from the experiment and those gained from calculation of correlations presented by other research works. The correlations used in a comparison with experimental results are shown in Table 3. The conditions of comparison are nanofluids volume concentration of 1 vol.% and inlet temperature of 30 °C, which complies with the conditions used by Azmi et al. [28] in their experiment and their

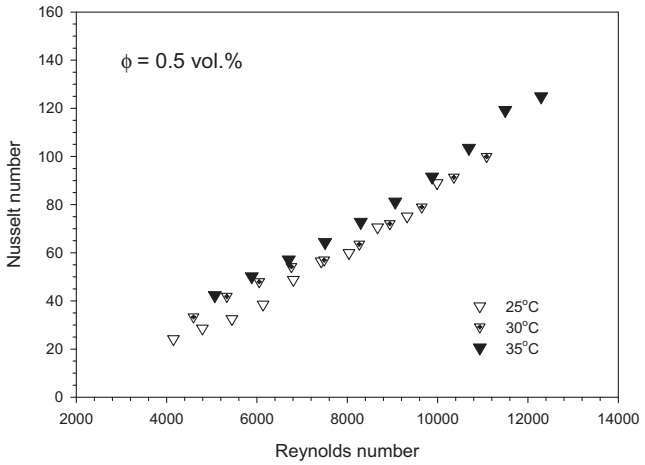


**Fig. 6.** Experimental Nusselt number for $SiO_2$/water nanofluids versus Reynolds number at volume concentration of 0.5 vol.%.

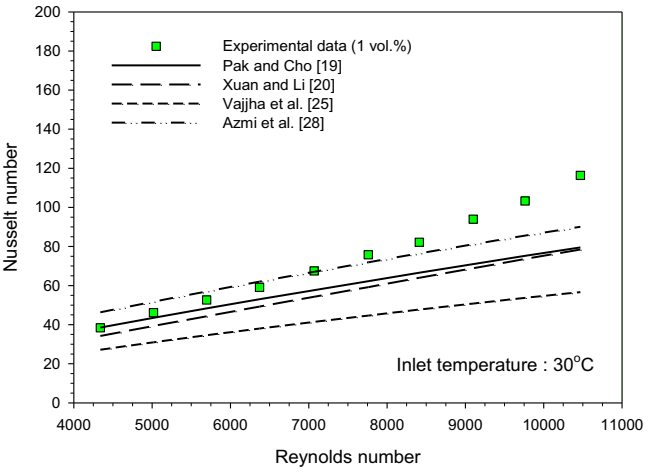


**Fig. 7.** Comparison of Nusselt number between the measured data and calculated values from nanofluid correlations.

calculated correlations. It can be seen that the experimental results are close to the values predicted by correlations of Azmi et al. [28] at Reynolds number lower than 9000. However, at Reynolds number higher than 9000, there is certain differences. This may results from the fact that the correlations derived from experimental results that used 22 nm nanoparticles whereas the values from present experimental results derived from 7 nm nanoparticles. The higher Nusselt number caused by smaller particles' diameter may result from the smaller specific surface area of particles than those of larger particles. So, the space between base fluid and nanoparticles becomes smaller and, as a result, heat could be better transferred from particles through base fluid to other particles. This difference could be obviously seen at higher Reynolds number.

On the other hand, the correlations proposed by Pak and Cho [19], Xuan and Li [20] could not predict Nusselt number because these correlations were not derived from experimental results that used $SiO_2$ nanoparticles. Similarly, even though the correlations presented by Vajjha et al. [25] were derived from experimental results that used $SiO_2$ nanoparticles, the base fluid was not water. Consequently, the experimental results are so different, when compared to the values predicted by these correlations, that the Nusselt number could not predicted accurately. Therefore, this research proposes a correlation to predict the Nusselt number as follows:

$$Nu_{nf} = f(Re_{nf}, Pr_{nf}, \phi, T_{in}) \tag{16}$$

From the above equation, the equation used to predict Nusselt number of $SiO_2$/water nanofluids is as follows:

$$Nu_{nf} = 0.001142\, Re_{nf}^{1.26}\, Pr_{nf}^{-0.19}(1+\phi)^{14.45}(T_{in}/25)^{-0.4} \tag{17}$$

A comparison between Nusselt number gained from the experiment and the one gained from prediction of the proposed correlation is shown in Fig. 8, with an error rate of ±10% for most data. It can be seen that the values gained from the prediction, compared to the values gain from the experiment, are sufficiently accurate to be used in predicting Nusselt number of $SiO_2$/water nanofluids. The condition of using this correlation includes volume concentration of not more than 2%, Reynolds number range between 3800 and 12,000, and inlet temperatures between 25 and 35 °C.

### 5.2. Pressure drop

Apart from its ability in heat transfer, another important factor that has to be considered in the practical application of nanofluids is pressure drop. A relationship between pressure drops in terms of mass flow rate at different volume concentrations is shown in Fig. 9. The experimental results indicate that the pressure drop increases when the mass flow rate increases, and it also increases slightly when the concentration increases. Similarly, Fig. 10 shows the relationship between friction factor and Reynolds number at different concentrations. As seen, friction factor decreases when Reynolds number increases. Similarly, when the concentration increases, the friction factor also increases slightly when compared to base fluid at the same Reynolds number. According to Blasius [40] an equation can be used to calculate pressure drop of fluid flowing through smooth surface circular pipe ($\Delta P = 0.158 L\rho^{3/4}\mu^{1/4}D_i^{-5/4}u^{7/4}$). The above equation shows clearly that the pressure drop depends more on density than viscosity of fluid. The slight increase of pressure drop and friction factor of nanofluids at higher concentrations results from the fact that the $SiO_2$ nanoparticle used in this experiment has a density of 2200 kg/m$^3$, which is not high when compared to water used as a base fluids. Therefore, the pressure drop and friction factor at various concentrations increases only slightly when compared to the base fluid.

Effects of inlet temperature on pressure drop are shown in Fig. 11. As seen, when the inlet temperature decreases, the pressure drop increases slightly. This is because the decrease of inlet

**Table 3**
Convective heat transfer correlations for nanofluids.

| Investigators | Base fluid | Particle material | Equations |
|---|---|---|---|
| Pak and Cho [19] | Water | $Al_2O_3$, $TiO_2$ | $Nu_{nf} = 0.021\, Re_{nf}^{0.8}\, Pr_{nf}^{0.5}$ |
| Xuan and Li [20] | Water | Cu | $Nu_{nf} = 0.0059\left(1 + 7.628\phi^{0.6886} Pe_d^{0.001}\right) Re_{nf}^{0.9238}\, Pr_{nf}^{0.4}$ |
| Vajjha et al. [25] | EG-water (40:60) | $Al_2O_3$, CuO, $SiO_2$ | $Nu_{nf} = 0.065(Re^{0.65} - 60.22)(1 + 0.0169\phi^{0.15})Pr^{0.542}$ |
| Azmi et al. [28] | Water | $SiO_2$ | $Nu_{nf} = 0.00896 Pr_w^{1/3}(f_r/8)^{-3.606} Re^{0.7406}\left(0.1 + \frac{\phi}{100}\right)^{2.541} f_r = \left[\left(\frac{\rho_{nf}}{\rho_w}\right)^{1.3}\left(\frac{\mu_{nf}}{\mu_w}\right)^{0.3}\right]$ |

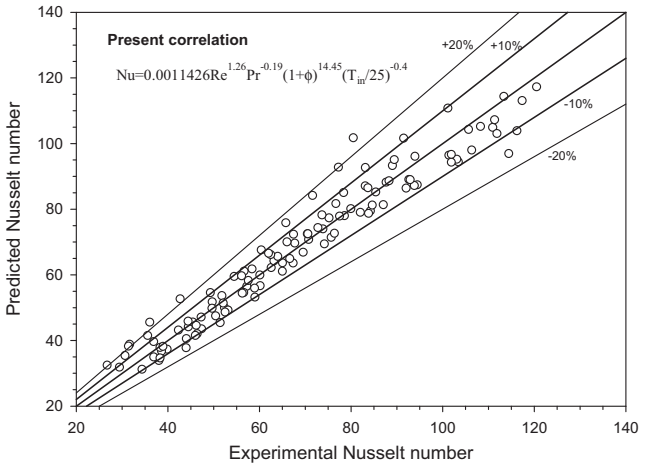


**Fig. 8.** Comparison of the Nusselt number of nanofluids between predicted values by presented correlation and Experimental data.

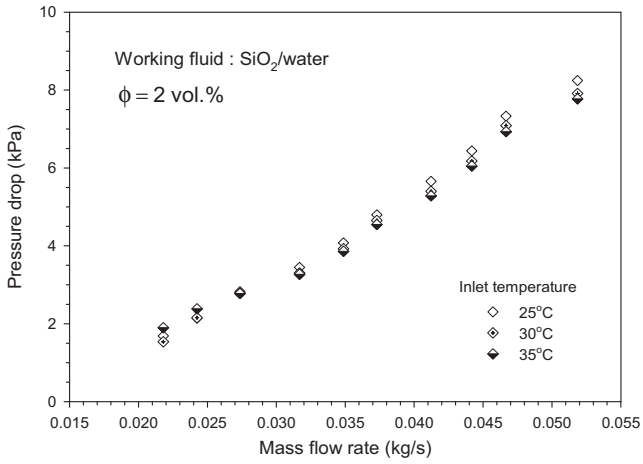


**Fig. 11.** Experimental pressure drop for $SiO_2$/water nanofluids versus mass flow rate at volume concentration of 2 vol.%.

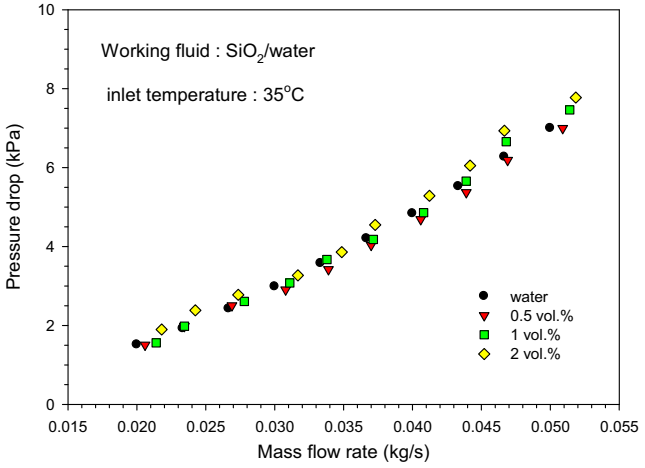


**Fig. 9.** Experimental pressure drop for water and $SiO_2$/water nanofluids versus mass flow rate at inlet temperature of 35 °C.

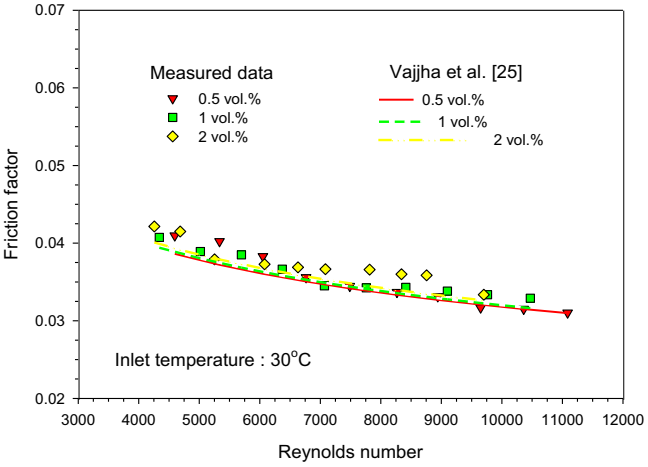


**Fig. 12.** Comparison of friction factor between the measured data and calculated values from nanofluid correlations.

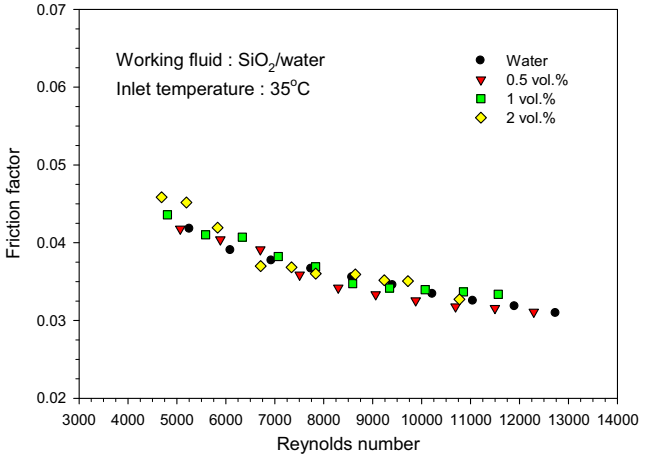


**Fig. 10.** Experimental friction factor for water and $SiO_2$/water nanofluids versus Reynolds number at inlet temperature of 35 °C.

temperature makes viscosity of nanofluids increases. However, effects of viscosity on pressure drop appears only slightly when compared to density.

Fig. 12 compares the values gained from the present experiments and the values gained from the prediction of correlation proposed by Vajjha et al. [25] as shown below:

$$f_{nf} = 0.316 Re_{bf}^{-0.25} \left(\frac{\rho_{nf}}{\rho_{bf}}\right)^{0.797} \left(\frac{\mu_{nf}}{\mu_{bf}}\right)^{0.108} \quad (18)$$

It can be seen that the friction factor gained from the experiments is rather different when compared to the one predicted from the correlation. This is because the proposed correlation derived from experimental results that used other kinds of nanoparticles in place of $SiO_2$, and the base fluid was not water, but a mixture between water–ethylene glycol at a ratio of 60:40.

The equation for predicting pressure drop in a form of dimensionless variables is:

$$f_{nf} = 0.527 Re_{nf}^{-0.3} (1+\phi)^{4.892} \quad (19)$$

The scope of this equation is in temperature range of 25–35 °C and volume concentration between 0 and 2%.

Fig. 13 shows a comparison between Nusselt number gained from the experiment and that gained from prediction with the proposed correlation (Eq. (19)). It can be seen that the predicted value and the experimental value are accurate in a range of ±10%. Thus, it

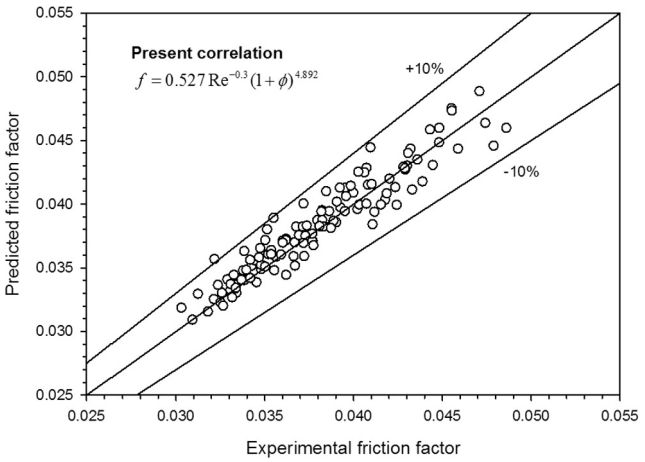


**Fig. 13.** Comparison of the Nusselt number of nanofluids between predicted values by presented correlation and experimental data.

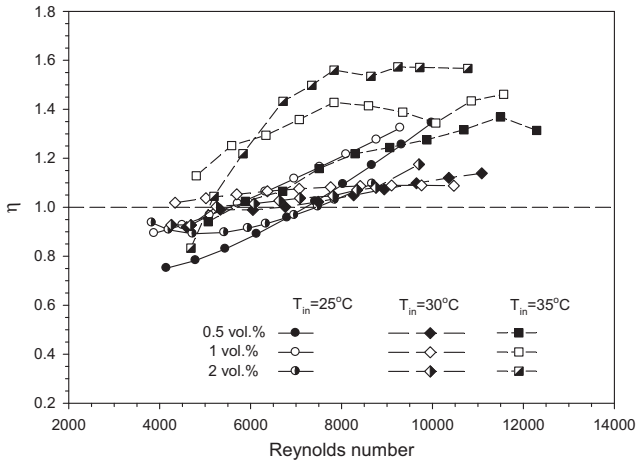


**Fig. 14.** Performance index (η) versus Reynolds number.

could be said that the proposed equation could be used to accurately predict friction factor of $SiO_2$/water nanofluids.

### 5.3. Efficiency index

In comparing heat transfer ability of heat exchanger, heat transfer rate is not the only factor to consider. Another important factor is pressure drop. The increase of heat transfer ability with any method is considered unsuitable if the pressure drop also increase immensely, even though more amount of heat could be transferred. Therefore, in a comparison of heat transfer ability of nanofluids and base fluids in this study, an efficiency index (η) is defined with the equation below:

$$\eta = \left(\frac{Nu_{nf}/Nu_w}{f_{nf}/f_w}\right) \tag{20}$$

It should be noted that in some studies, efficiency index is also called performance index.

As shown in Fig. 14, it can be clearly seen that, at inlet temperature of 35 °C, the efficiency index is outstandingly higher than other factors. This is because at high inlet temperatures, the thermal conductivity of nanofluids also increases which, in turn, leads to better heat transfer. On the contrary, the decrease in viscosity of nanofluids will make the pressure drop decreases, at the same Reynolds number. It is also noticeable that at Reynolds numbers greater than 9000 the efficiency index remains constant. The maximum number is approximately 1.6 at volume concentration of 2 vol.% and inlet temperature of 35 °C.

## 6. Conclusion

The heat transfer and flow characteristics of $SiO_2$/water nanofluids with particle volume fractions of 0.5, 1 and 2% flowing through a circular stainless tube were experimented. The effects of particle volume concentration, inlet temperature and mass flow rate on heat transfer and pressure drop were compared with water. The main findings are summarized as follows.

- The ability in heat transfer of nanofluids is better than that of base fluid and increases with increasing concentration, inlet temperature and mass flow rate.
- When volume concentration and inlet temperature rise, the Nusselt number also increases. The increment in Nusselt number for $SiO_2$/water nanofluids for volume concentration of 2%, inlet temperature of 35 °C and Reynolds number of about 11,000 is found to be approximately 35% over than that of base fluid.
- Friction factor of nanofluids slightly increases with increasing the concentration, but decreases as the inlet temperature rises. The friction factor increases when compared to the base fluid at low Reynolds number.
- Correlations for predicting Nusselt number and friction factor for $SiO_2$/water nanofluids are expressed as $Nu_{nf} = 0.001142\,Re_{nf}^{1.26}\,Pr_{nf}^{-0.19}(1+\phi)^{14.45}\left(\frac{T_{in}}{25}\right)^{-0.4}$ and $f_{nf} = 0.527\,Re_{nf}^{-0.3}(1+\phi)^{4.892}$, respectively. Most experimental data have a relative difference of less than ±10% when compared to the value calculated from the above correlations.
- The efficiency index reached its maximum quantity (i.e. 1.6) at Reynolds numbers higher than 9000, the volume concentration of 2%, and inlet temperature of 35 °C.
- The minimum values of efficiency index were obtained for Reynolds numbers less than 7000, the volume fraction of 0.5%, and inlet temperature of 25 °C.

In future studies, the effects of magnetic field, electrical field, installing fins with different shapes and materials on the internal wall, and using hybrid nanofluids on the flow and heat transfer patterns can be investigated.

## Acknowledgments

The authors acknowledge the financial support provided by the "Research Chair Grant" National Science and Technology Development Agency (NSTDA), the Thailand Research Fund (TRF), the National Research University Project (NRU) and King Mongkut's University of Technology Thonburi through the "KMUTT 55th Anniversary Commemorative Fund".

## References

[1] W. Duangthongsuk, S. Wongwises, Measurement of temperature-dependent thermal conductivity and viscosity of $TiO_2$-water nanofluids, Exp. Thermal Fluid Sci. 33 (2009) 706–714.
[2] O. Mahian, A. Kianifar, S. Wongwises, Dispersion of ZnO nanoparticles in a mixture of ethylene glycol–water, exploration of temperature-dependent density, and sensitivity analysis, J. Cluster Sci. 24 (4) (2013) 1103–1114.
[3] J. Cai, X. Hu, B. Xiao, Y. Zhou, W. Wei, Recent developments on fractal-based approaches to nanofluids and nanoparticle aggregation, Int. J. Heat Mass Transf. 105 (2017) 623–637.
[4] M. Hemmet Esfe, S. Saedodin, O. Mahian, S. Wongwises, Thermal conductivity of $Al_2O_3$/water nanofluids: measurement, correlation, sensitivity analysis, and

comparisons with literature reports, J. Therm. Anal. Calorim. 117 (2014) 675–681.
[5] M. Hemmet Esfe, S. Saedodin, S. Wongwises, D. Toghraie, An experimental study on the effect of diameter on thermal conductivity and dynamic viscosity of Fe/water nanofluids, J. Therm. Anal. Calorim. 119 (2015) 1817–1824.
[6] C.J. Ho, D.S. Chen, W.M. Yan, O. Mahian, Buoyancy-driven flow of nanofluids in a cavity considering the Ludwig-Soret effect and sedimentation: Numerical study and experimental validation, Int. J. Heat Mass Transf. 77 (2014) 684–694.
[7] I. Rashidi, O. Mahian, G. Lorenzini, C. Biserni, S. Wongwises, Natural convection of $Al_2O_3$/water nanofluid in a square cavity: effects of heterogeneous heating, Int. J. Heat Mass Transf. 74 (2014) 391–402.
[8] M.H. Esfe, M. Akbari, A. Karimipour, M. Afrand, O. Mahian, S. Wongwises, Mixed convection flow and heat transfer in an inclined cavity equipped to a hot obstacle using nanofluids considering temperature-dependent properties, Int. J. Heat Mass Transf. 85 (2015) 656–666.
[9] O. Mahian, A. Kianifar, A.Z. Sahin, S. Wongwises, Performance analysis of a minichannel-based solar collector using different nanofluids, Energy Convers. Manage. 88 (2014) 129–138.
[10] P. Nitiapirak, O. Mahian, A.S. Dalkilic, S. Wongwises, Performance characteristics of a microchannel heat sink using $TiO_2$/water nanofluid and different thermophysical models, Int. Commun. Heat Mass Transfer 47 (2013) 98–104.
[11] S.Z. Heris, M.B. Pour, O. Mahian, S. Wongwises, A comparative experimental study on the natural convection heat transfer of different metal oxide nanopowders suspended in turbine oil inside an inclined cavity, Int. J. Heat Mass Transf. 73 (2014) 231–238.
[12] K. Bashirnezhad, S. Bazri, M.R. Safaei, M. Goodarzi, M. Dahari, O. Mahian, A.S. Dalkılıç, S. Wongwises, Viscosity of nanofluids: A review of recent experimental studies, Int. Commun. Heat Mass Transfer 73 (2016) 114–123.
[13] S.S. Meibodi, A. Kianifar, H. Niazmand, O. Mahian, S. Wongwises, Experimental investigation on the thermal efficiency and performance characteristics of a flat plate solar collector using $SiO_2$/EG–water nanofluids, Int. Commun. Heat Mass Transfer 65 (2015) 71–75.
[14] F. Yazdanifard, M. Ameri, E. Ebrahimnia-Bajestan, Performance of nanofluid-based photovoltaic/thermal systems: A review, Renew. Sustain. Energy Rev. 76 (2017) 323–352.
[15] O. Mahian, A. Kianifar, S.A. Kalogirou, I. Pop, S. Wongwises, A review of the applications of nanofluids in solar energy, Int. J. Heat Mass Transf. 57 (2013) 582–594.
[16] W. Daungthongsuk, S. Wongwises, A critical review of convective heat transfer of nanofluids, Renew. Sustain. Energy Rev. 11 (2007) 797–817.
[17] A.K. Hussein, Applications of nanotechnology in renewable energies-A comprehensive overview and understanding, Renew. Sustain. Energy Rev. 42 (2015) 460–476.
[18] O. Mahian, A. Kianifar, S.Z. Heris, D. Wen, A.Z. Sahin, S. Wongwises, Nanofluids effects on the evaporation rate in a solar still equipped with a heat exchanger, Nano Energy 36 (2017) 134–155.
[19] B.C. Pak, Y.I. Cho, Hydrodynamic and heat transfer study of dispersed fluids with submicron metallic oxide particles, Exp. Heat transfer 11 (1998) 151–170.
[20] Y. Xuan, Q. Li, Investigation on convective heat transfer and flow features of nanofluids, J. Heat Transfer 125 (2003) 151–155.
[21] W. Duangthongsuk, S. Wongwises, An experimental study on the heat transfer performance and pressure drop of $TiO_2$-water nanofluids flowing under a turbulent flow regime, Int. J. Heat Mass Transf. 52 (2009) 2059–2067.
[22] A.A. Abbasian Arani, J. Amani, Experimental investigation of diameter effect on heat transfer performance and pressure drop of $TiO_2$-water nanofluid, Exp. Thermal Fluid Sci. 44 (2013) 520–533.
[23] M. Karimzadehkhouei, S.E. Yalcin, K. Sendur, M.P. Menguc, A. Kosar, Pressure drop and heat transfer characteristics of nanofluids in horizontal microtubes under thermally developing flow conditions, Exp. Thermal Fluid Sci. 67 (2015) 37–47.
[24] D.P. Kulkarni, P.K. Namburu, H. Ed Bargar, D.K. Das, Convective heat transfer characteristics of $SiO_2$-ethylene glycol/water nanofluids, Heat Transfer Eng. 29 (2008) 1027–1035.
[25] R.S. Vajjha, D.K. Das, D.P. Kulkarni, Development of new correlations for convective heat transfer and friction factor in turbulent regime for nanofluids, Int. J. Heat Mass Transf. 53 (2010) 4607–4618.
[26] S. Ferrouillat, A. Bontemps, J.P. Ribeiro, J.A. Gruss, O. Soriano, Hydraulic and heat transfer study of $SiO_2$/water nanofluids in horizontal tubes with imposed wall temperature boundary conditions, Int. J. Heat Fluid Flow 32 (2011) 424–439.
[27] S. Ferrouillat, A. Bontemps, O. Poncelet, O. Soriano, J.A. Gruss, Influence of nanoparticle shape factor on convective heat transfer and energetic performance of water-based $SiO_2$ and ZnO nanofluids, Appl. Therm. Eng. 51 (2013) 839–851.
[28] W.H. Azmi, K.V. Sharma, P.K. Sarma, R. Mamat, S. Anuar, V.D. Rao, Experimental determination of turbulent forced convection heat transfer and friction factor with $SiO_2$ nanofluid, Exp. Thermal Fluid Sci. 51 (2013) 103–111.
[29] W.H. Azmi, K. Abdul Hamid, Rizalman Mamat, K.V. Sharma, M.S. Mohamad, Effects of working temperature on thermos-physical properties and forced convection heat transfer of $TiO_2$ nanofluids in water – ethylene glycol mixture, Appl. Therm. Eng. 106 (2016) 1190–1199.
[30] A. Merilainen, A. Seppala, K. Saari, J. Seitsonen, J. Roukolainen, S. Puisto, N. Rostedt, T. Ala-Nissila, Influence of particle size and shape on turbulent heat transfer characteristics and pressure losses in water-based nanofluids, Int. J. Heat Mass Transf. 61 (2013) 439–448.
[31] R. Matinez-Cuenca, R. Mondragon, L. Hernandez, C. Segarra, J.C. Jarque, T. Hibiki, J.E. Julia, Forced-convective heat-transfer coefficient and pressure drop of water-based nanofluids in a horizontal pipe, Appl. Therm. Eng. 98 (2016) 841–849.
[32] L. Godson, B. Raja, D. Mohan Lal, S. Wongwises, Enhancement of heat transfer using nanofluids-An overview, Renew. Sustain. Energy Rev. 14 (2010) 629–641.
[33] J. Sarkar, A critical review on convective heat transfer correlations of nanofluids, Renew. Sustain. Energy Rev. 15 (2011) 3271–3277.
[34] L.S. Sundar, M.K. Singh, Convective heat transfer and friction factor correlations of nanofluid in a tube and with inserts: A review, Renew. Sustain. Energy Rev. 20 (2013) 23–35.
[35] R.S. Vajjha, D.K. Das, Specific heat measurement of three nanofluids and development of new correlations, J. Heat Transfer 131 (2009) 071601.
[36] K.V. Sharma, P.K. Sarma, W.H. Azmi, R. Mamat, K. Kadirgama, Correlations to predict friction and forced convection heat transfer coefficients of water based nanofluids for turbulent flow in a tube, Int. J. Microscale Nanoscale Therm. Fluid Transport Phenom. (Special Issue in Heat and Mass Transfer in Nanofluids) 3 (4) (2012) 1–25.
[37] F.W. Dittus, L.M.K. Boelter, Heat transfer in automobile radiators of the tubular type, Univ. California Publ. Eng. 2 (1930) 433–461.
[38] C.A. Sleicher, M.W. Rouse, A convenient correlation for heat transfer to constant and variable property fluids in turbulent pipe flow, Int. J. Heat Mass Transf. 18 (1975) 677–683.
[39] V. Gnielinski, New equations for heat and mass transfer in turbulent pipe and channel flow, Int. Chem. Eng. 16 (1976) 359–368.
[40] P.R.H. Blasius, Das Aehnlichkeitsgesetz bei Reibungsvorgangen in Flüssigkeiten, Mitteilungen uber Forschungsarbeuten auf dem Gebiete des Ingenieurwesens 131 (1913).
[41] S.E. Haaland, Simple and explicit formulas for the friction factors in turbulent pipe flow, J. Fluids Eng. (1983) 89–90.